Fast molecular reorientations in liquid crystals

J. R. Lalanne, C. Destrade, H. T. Nguyen, and J. P. Marcerou
Centre de Recherche Paul Pascal, Centre National de la Recherche Scientifique, Avenue A. Schweitzer, 33600 Pessac, France
(Received 10 December 1990)

We report investigations on fast individual molecular reorientations in isotropic, nematic (N), and smectic-A (Sm-A) phases of chiral, achiral, and racemic liquid crystals. These motions, in the $10^{-11}-10^{-10}$ s range, are probed by the degenerate four-waves-mixing technique and compared to results obtained by other techniques. In homeotropic N and Sm-A phases of achiral compounds and racemic mixture, the individual reorientation time about the long molecular axis is found to be unchanged down to the Sm-$A \rightarrow$Sm-C transition, but increases by a factor of about 3 with a chiral compound. A quantitative comparison between theoretical prediction and experiment is presented. This result is in agreement with our previous work [Phys. Rev. Lett. **62**, 3049 (1989)] and does not support the recent theoretical work by Brand *et al.* [Phys. Rev. Lett. **64**, 1309 (1990)] as well as the results of the dielectric spectroscopy experiments of Kremer *et al.* [Phys. Rev. A **42**, 3667 (1990)] performed at inappropriately low frequencies.

PACS number(s): 64.70.Md

I. INTRODUCTION

Mainly due to the importance of their technological applications, the orientational properties of liquid crystals have been the object of intense research in the past two decades. Experimental results show that the rotational reorientation times belong to two very different classes. The first one, extensively studied in the 1970s [1–5] in isotropic phases, collects what can be viewed as the order-parameter [6] relaxation time. The times belonging to the first class are associated with *cooperative* rotations, i.e., with orientational fluctuations of molecules under the influence of the mean field created by long-range intermolecular interactions, and lie in the $10^{-10}-10^{-5}$ s range. The second class, which is the object of the present work, concerns *pseudoindividual* orientational fluctuations [7] of molecules. It has been theoretically known [8] for fifteen years that there exist many of these reorientational times which lie in the $10^{-12}-10^{-9}$ s range. During the past two decades, both classes have been extensively studied by techniques such as dielectric spectroscopy (DS) [8], far-infrared spectroscopy (FIR) [8], quasielastic neutron spectroscopy (QNS) [9–11], electron spin relaxation (ESR) [12], and "optical" techniques which are well suited for the study of fast phenomena. Moreover, the latter give direct information about molecular reorientations. Since then many optical investigations in liquid crystals have been published starting with the pioneering work in Rayleigh scattering (RS) of Amer in 1975 [13], continuing with the optical Kerr effect (OKE) [14], holographic grating (HG) [15], and degenerate four-wave-mixing (DFWM) [16,17] approaches. All these techniques have been used not only to study isotropic phases but also to explore fast rotational dynamics in thin oriented liquid-crystal samples.

We report herein the results of an experimental investigation on reorientational times, using DFWM in the picosecond range, and performed on samples (200- and 500-μm thick) of liquid crystals in the isotropic (I), homeotropic nematic (N), and smectic-A (Sm-A) phases. Buth achiral, chiral, and racemic mixtures are considered.

The DFWM investigation is presented in Sec. II, while Sec. III describes the experimental setup and the preparation of the oriented liquid crystal. Finally, the experimental results for the three investigated phases of four compounds are given and discussed in Sec. IV.

II. THE DFWM INVESTIGATION

The experimental geometry is given in Fig. 1. It is similar to the one already used for investigations of cooperative orientational fluctuations in the isotropic phases of nematogens [16]. A mode-locked YAG (where YAG represents yttrium aluminum garnet) laser system produces single pulses, frequency doubled, to give 1-mJ, 25-ps, Fourier-transform-limited pulses at 532 nm. The laser is split into three beams, denoted by pump 1, pump 2, and probe, linearly polarized as shown in Fig. 1. Pump 1 and probe can be delayed in time in the picosecond range (pump 2 is taken as the time reference). It has been known for some time [18] that when three laser pulses spatially and temporally overlap in a material having a large nonlinear susceptibility $\chi^{(3)}(-\omega,\omega,\omega,-\omega)$ at the laser frequency ω, a phase-conjugate backward wave BW is generated in the direction of the probe. The number of photons carried by the BW pulse and detected by an integrator is given, in the slowly varying envelope approximation, by [19]

$$I_{\mathrm{BW}} \propto \int_{-\infty}^{+\infty} |P^{(3)}(t)|^2 dt \ , \tag{1}$$

where $P^{(3)}(t)$ is the third-order polarization of the medium (we have omitted the spatial dependence). It can be written as [20]

$$P^{(3)}(t) \propto E^*_{pr}(t-\tau_{pr}) \int_{-\infty}^{t} C(t-t') E_{pu,1}(t'-\tau_{pu}) E_{pu,2}(t') dt' + E_{pu,2}(t) \int_{-\infty}^{t} C(t-t') E^*_{pr}(t'-\tau_{pr}) E_{pu,1}(t'-\tau_{pu}) dt' + E_{pu,1}(t-\tau_{pu}) \int_{-\infty}^{t} C(t-t') E^*_{pr}(t'-\tau_{pr}) E_{pu,2}(t') dt' \ . \quad (2)$$

$C(t-t')$ is the time-dependent response of the medium and τ_{pu} and τ_{pr} are, respectively, the (pump 1-pump 2) and (probe-pump 2) delays. $E(t)$ denotes the time dependence of the electric field of the light wave.

Equation (2) describes the spatial modulation of the refractive index of the medium due to the interference between incident waves. The modulation pattern can be viewed as a volume grating, impressed in the medium by two of the three waves, which scatters the third one. As already stated [21], any grating built between pump 1 and pump 2 [first term in Eq. (1)] does not markedly contribute to the BW intensity because of the phase mismatch in the BW direction. The second and third terms describe matched diffraction of pump 2 (respectively, pump 1) by the grating due to the interference between probe and pump 1 (respectively, pump 2).

If λ is the laser wavelength and θ the angle between the wave vectors of probe and pump 1 (it is close to 7°), the gratings have periods Λ and Λ' given by

$$\Lambda = \frac{\lambda}{2}\sin\frac{\theta}{2} \quad \text{(for probe-pump 1)} \ , \qquad \Lambda' = \frac{\lambda}{2}\cos\frac{\theta}{2} \quad \text{(for probe-pump 2)} \ . \quad (3)$$

Note that $\Lambda \gg \Lambda'$.

Let us point out here that due to the crossed polarizations of probe and pumps (Fig. 1), all the intensity gratings are avoided in our work [22]. The beam interferences only create gratings (also called polarization gratings).

We must now discuss the physical mechanisms which can contribute to the BW generation. They can be classified into two groups. The first can be called the "slow" group and includes thermal heating [20] and electrostriction [23]. The lack of intensity gratings in our polarization geometry allows us to neglect it. The second ("fast") one comes from electronic deformation [4] and molecular orientation [24] which have already been shown to play the main part in the chosen polarization [16] and to contribute to the generated signal. Both are also known to play the main part in OKE [25] experiments.

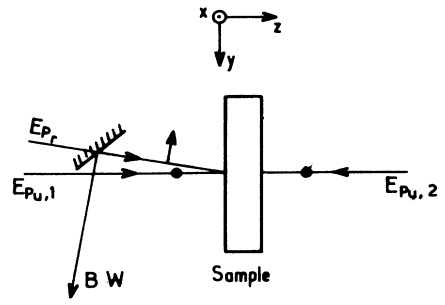

FIG. 1. Experimental geometry.

The DFWM experiment, in the crossed polarizations configuration, thus appears equivalent to the OKE technique. However, the former presents the important advantage—due to the energy transfer occurring during the mixing process—of generating intense BW signals, thus allowing investigations on thin samples (some hundreds of microns), which cannot be studied by the OKE technique.

In usual liquids composed of molecules with large anisotropy, Γ^2, of the first-order polarizability [26] (CS_2, benzene, nitrobenzene, etc.), the contribution of electronic deformation is very small [27] and the molecular orientation mechanism is largely dominant. Liquid-crystal molecules are known to have very large Γ^2. For instance, in the cyanobiphenyl series, Γ^2 up to 900×10^{-48} cm^6 have been measured [28] for $\lambda=510$ nm (30 times larger than that of benzene). It seems then probable that the electronic contribution remains small in liquid-crystal investigations.

This prediction has been confirmed experimentally. Recent experiments performed on liquid crystals report small third-order polarizability [29] and show that the dominant nonlinearity, even for the short picosecond pulses, is due to molecular reorientation [30]. Moreover, one of the results presented here (see Sec. IV) exhibits a large variation of the nonlinearity *inside* the Sm-A phase, which is totally incompatible with the structure-independent deformation of the electronic clouds.

The electronic deformation contribution will therefore be neglected in our DFWM work [31]. This assumption allows us to specify the time-dependent response, $C(t)$ in Eq. (2), describing only pseudoindividual molecular reorientations. For homeotropic alignment (phases N and Sm-A; director in the Z direction of Fig. 1), the molecular reorientations are those about the *long molecular axis.* Under the assumption of a single relaxation, $C(t)$ may be characterized by

$$C(t) \propto \rho \mathcal{L} \frac{\Gamma_\perp^2}{kT\tau_R} \exp\left[-\frac{t}{\tau_R}\right] = \frac{A}{\tau_R}\exp\left[-\frac{t}{\tau_R}\right] \ , \quad (4)$$

where ρ is the number density of molecules, $\mathcal{L}$ a local-field correction factor [32], and τ_R the relaxation time for the reorientation. $\Gamma_\perp^2=(\alpha_{yy}-\alpha_{xx})^2$ describes the "restricted" anisotropy of the first-order polarizability (in plane anisotropy). $0x$ and $0y$ are assumed to be the principal axes of the first-order polarizability. $\Gamma_\perp=0$ in the case of optical "rodlike" molecules. It should be noted that the response function $C(t)$ is also a function of the wave-vector differences $k_{pu,1}-k_{pr}$ [second term of Eq. (2)] and of $k_{pu,2}-k_{pr}$ [third term of Eq. (2)], due to a coupling between reorientation and transverse momentum density. In liquid crystals, however, this coupling is as-

sumed to be small for the chosen geometry [16], therefore this k dependence will not be taken into account. In the case of I phases, Γ_1^2 previously defined [26], and τ_R must be considered as a *mean* reorientation time around all the axes of the molecule.

Let us now discuss the temporal shape of the incoming laser pulse $E(t)$ that must be included in Eq. (2). We assume, as already proposed [24], a phase-modulated pulse with a Gaussian envelope described by

$$E(t)=\epsilon(t)\exp[ia\epsilon^2(t)] \tag{5}$$

with

$$\epsilon(t)=\exp\left[-2(\ln 2)\left[\frac{t}{T}\right]^2\right],$$

where T characterizes the pulse duration and a the magnitude of the phase modulation.

T can be measured [19,33] and is known to be about 25 ps. However, the parameter a, which is connected to the coherence time of the pulse [34], is difficult to measure and probably has large fluctuations during the sampling time. We will see later how one can avoid this difficulty. As already mentioned, the last two terms of Eq. (2) are only important in our work. Figure 2 reports a computer simulation of the variations of $I_{\mathrm{BW}}(\tau_R;\tau_{pu};\tau_{pr})$ versus τ_{pu} in the simplified case when $a=0$ and $\tau_{pr}=0$.

Two very important points should be noted:

(i) The signal duration increases with τ_R. One could then determine accurately τ_R from the measurement of the signal width (method 1) provided T is much smaller than τ_R. This is not the case in this work where both τ_R and T are in the 10-ps range.

(ii) For $\tau_{pr}=\tau_{pu}=0$ (the three laser pulses reach the sample at the same time) the *amplitude* of the signal strongly decreases when τ_R increases. Figure 3 shows an attenuation factor of 25 in the range 10^{-12}–10^{-10} s.

It appears that the measurement of $I_{\mathrm{BW}}(\tau_R;0;0)$ will probably be a more relevant method to check the variations of the reorientation time τ_R in the expected range (method 2). Moreover, in this case, the phase modulation does not play any part because of the real nature of the products involved in Eq. (2):

$$\begin{aligned}E^*_{pr}(t')E_{pu,1}(t')&=E^*_{pr}(t')E_{pu,2}(t')\\&=E^*_{pu,1}(t')E_{pu,1}(t')\\&=E^*_{pu,2}(t')E_{pu,2}(t')\\&=|\epsilon(t')|^2=\exp\left[-4(\ln 2)\left[\frac{t'}{T}\right]^2\right].\end{aligned} \tag{6}$$

So the second method, i.e., plotting the variations of $I_{\mathrm{BW}}(\tau_R;0;\tau_{pr})$ versus τ_{pr} and taking the maximum occurring for $\tau_{pr}=0$, will be chosen. However, the consistency of the two methods will be evaluated later (see Sec. IV B).

III. EXPERIMENT

A. Apparatus (Fig. 4)

The YAG laser is simultaneously Q switched and mode located by an acousto-optic mode locker (Intra Action Corp. Model No. ML 70 B) coupled to passive dye mode

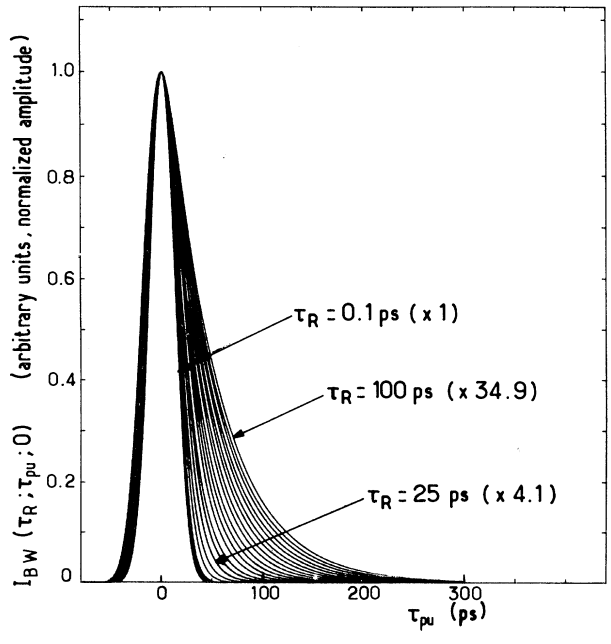

FIG. 2. Calculated $I_{\mathrm{BW}}(\tau_R,\tau_{pu},0)$ vs delay τ_{pu} between the two pump waves for some values of $\tau_R(\tau_{pr}=0)$. T and a are held fixed at, respectively, 25 ps and 0. The amplitude has been normalized to 1; it is in fact a steep decreasing function of τ_R as shown in Fig. 3.

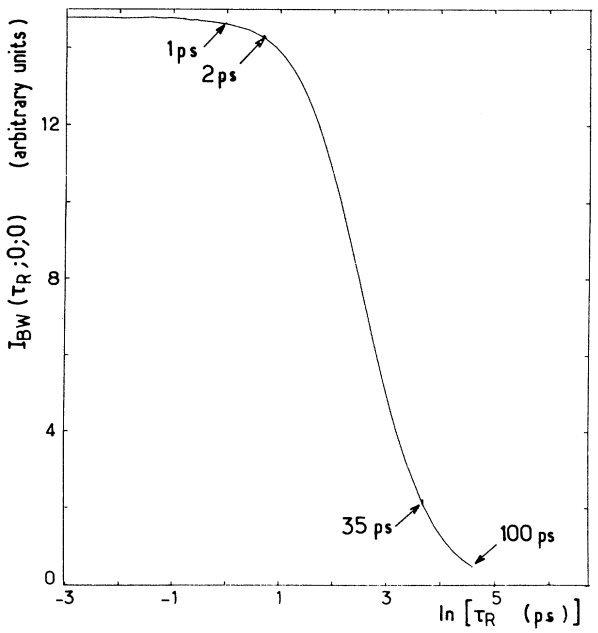

FIG. 3. Calculated amplitude of the signal $I_{\mathrm{BW}}(\tau_R,0,0)$ vs τ_R [second and third terms of Eq. (2)]. A and T are held fixed ($T=25$ ps); $a=0$.

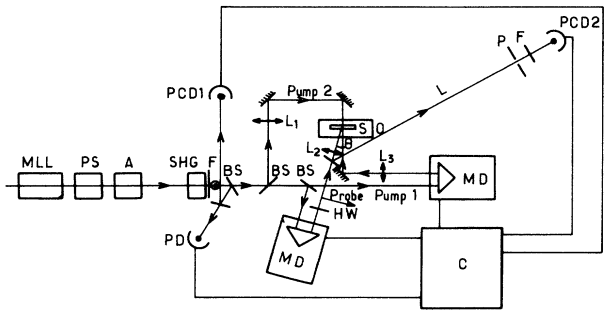

FIG. 4. Experimental setup: MLL, mode-locked laser; PS, pulse selector; A, double scan amplifier; SHG, second-harmonic generator; F, interference filters; $\lambda=530$ nm; BS, beam splitters; HW, half-wave plate $\lambda=530$ nm; S, sample; O, oven; PD, fast photodiode; PCD, photon counting device; C, computer; MD, mechanical delays; P, pinhole $\phi\simeq 5$ mm; $L\simeq 3$ m; $\theta\simeq 7°$; L_1, lens $f=50$ cm; L_2, lens $f=16$ cm; L_3, lens $f=40$ cm.

locking (Eastman Kodak No. 9740). A single pulse ($\lambda=1060$ nm; $T\simeq 25$ ps) is selected from the first half of the pulse train by a single pulse selector (Quantel Model No. SPS 411) at a frequency rate of 1 Hz. It is amplified by a double passing homemade YAG amplifier. A second-harmonic generator (Quantel Model No. DO 35) generates single green ($\lambda=530$ nm) pulses of about 1 mJ energy. These pulses are monitored by a fast photodiode, coupled to a digitizer (Tektronix Model No. 7912 AD), that triggers the signal acquisition by a computer (DEC LSI 11 and VAX 8600) which drives the experiment.

The two pumps and the probe waves are separated by several beam splitters and are slightly focused on the sample placed inside an oven, the temperature of which is regulated to ± 0.01 K. The probe and the first pump can be delayed by mechanical drivers (Microcontrôle). The angle θ between probe and pump 1 is close to 7°. The distance length L between the sample and the photon counting device (PCD2 in Fig. 4) is about 3 m. This distance, together with the pinhole diameter (about 5 mm) placed in front of the detector, largely reduces the spurious signals coming from all the optical components of the setup, thus affording the detection of the DFWM signal on a very weak background. PCD1 monitors the intensity of the incoming pulse, allowing the necessary check of the I_{BW} dependence with the third power of the laser intensity. Because of this power law, the laser intensity stability has been carefully controlled. An accurate adjustment of cavity length, as required by the active mode locking, yielded, after selecting the single pulse, a ratio between the standard deviation and the signal of about 0.05 (over periods of several hours).

B. Compounds

Phase transition temperatures of studied compounds are listed in Table I. Compounds 1 and 2 were purchased from BDH Chemicals Ltd. and Merck and used without further purification. The Merck mixture (2) has a compensated helical pitch in the N^* phase that diverges close to the Sm-A phase transition.

C. Sample preparation

Since a homeotropic alignment is required to work in the Sm-A phase (for all compounds) or in the nematic phase (compound 1), the inner faces of two fused silica ($\phi=25$ mm) windows were coated with octadecyl triethoxysilane. The thickness of the cell can be 200 or 500 μm. It is filled with the compound in the I phase. Then, the temperature is slowly decreased down to the Sm-A phase (a few hours). Such a procedure can be successfully used for compounds 1 and 3 (Table I). In the case of chiral molecules [35] (compounds 2 and 4), the samples turn out to give poor optical quality in the Sm-A phase. The alignment is improved by a static magnetic induction of about 3000 G, perpendicular to the surfaces.

The optical quality is carefully controlled by measurement of the extinction ratio between crossed polarizers both normal to the wave vector of the beam and to the director. Sm-C and Sm-C^* phases are opaque and cannot be studied. We have also controlled that, as expected, optical activity of chiral compounds [36] does not appreciably rotate polarizations of the three incoming waves.

IV. RESULTS AND DISCUSSION

A. Preliminary work on carbon disulfur

We have chosen CS_2, because of its importance as a nonlinear standard, to check out setup. In the liquid state the anisotropy of the first-order polarizability is 117×10^{-48} cm^6 for $\lambda=546$ nm at room temperature [37]. The orientational relaxation time is near 2 ps [38]. The amplitude of the signal in CS_2 is one order of magnitude larger than it is in all the liquid crystals we studied. Figure 5 shows the registered I_{BW} signal and the fit of the data to the equation [second and third terms of Eq. (2)]

$$I_{BW}(\tau_R;0;\tau_{pr})=\frac{A^2}{\tau_R^2}\int_{-\infty}^{+\infty}\epsilon^2(t)\left[\int_{-\infty}^{+\infty}\exp-\left[\frac{(t-t')}{\tau_R}\right]\epsilon(t'-\tau_{pr})\epsilon(t')dt'\right]^2 d\ . \tag{7}$$

With fixed T (25 ps) and τ_R (2 ps), the agreement seems correct. Moreover, the pulse duration at half amplitude can be controlled in the following way. In the case $\tau_R \ll T$, (6) can easily we written in the limit $\tau_R\rightarrow 0$:

$$I_{BW}(\tau_R\rightarrow 0;0;\tau_{pr})\simeq A^2 T\left[\frac{\pi}{12\ln 2}\right]^{1/2}\exp\left\{-\left[\frac{8}{3}(\ln 2)\left[\frac{\tau_{pr}}{T}\right]^2\right]\right\}. \tag{8}$$

At half amplitude, the pulse duration is $2\tau_{pr,1/2}=T\sqrt{3}/2$. We find it to be $\simeq 30.6$ ps, in agreement with the 32 ps directly read in the curve of Fig. 5.

We will now report on and discuss results obtained with the different compounds.

B. Compound 1 (8CB)

The first observation concerns the amplitude of the generated back wave. For the three phases Sm-A, N, and I, the amplitude is smaller than for CS_2. In spite of the great difficulty to change samples without geometric modification of the superposition of the three incoming waves, we have obtained a mean ratio for the signals given by CS_2 and 8CB of about 18 ± 2 (8CB being at 31.5 °C, i.e., in the Sm-A phase). One must evaluate the ratio $(A_{CS_2}/A_{8CB})^2$ [A is given by Eq. (4)] in order to determine whether or not it is at the origin of the experimental observation. With the numerical values [39] $\rho_{CS_2}=1.0\times10^{22}$ cm^{-3}, $\rho_{8CB}=2.0\times10^{21}$ cm^{-3}, $n_{CS2}=1.63$, $n_{8CF}=1.56$, $\Gamma^2_{CS2}=117\times10^{-48}$ cm^6, $\Gamma^2_{\perp 8CB}=441\times10^{-48}$ cm^6, and taking [16] $\mathcal{L}=(n^2+2/3)^4$, we find a ratio of about 2.8 i.e., 6.4 times smaller than the measured one. Therefore, the slowing down factor, due to the larger τ_R for 8CB as compared to CS_2, is about 6.4. If one refers to Fig. 3, and to the 2-ps reorientational time of CS_2, one finds for 8CB $\tau_R\sim35$ ps. Figure 2 shows that this relaxation time only gives a very small increase of the width at half maximum of the signal $I_{BW}(\tau_R;\tau_{pu};0)$ versus τ_{pu} ($\tau_{pu,1/2}$ is found close to 26 ps).

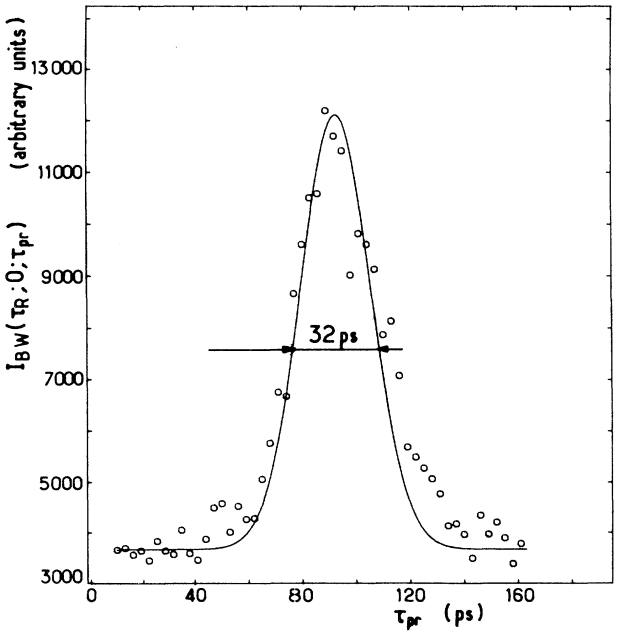

FIG. 5. Variation of the signal intensity $I_{BW}(\tau_R;0,\tau_{pr})$ with delay τ_{pr} between probe and pump waves. Compound, CS_2; $t=(25.0\pm0.1)$°C; thickness of the sample, 200 μm; $T=25$ ps; ○, experimental points; —, fit of Eq. (6) with $\tau_R=2.0$ ps (held fixed).

TABLE I. The studied compounds.

No.	Compound	Origin	Molecular formula	Chirality	Ferro-electricity	T(°C) $S_C\rightleftarrows S_a$ or $S_C^*\rightleftarrows S_A$	T(°C) $S_A\rightleftarrows N$ or $S_A\rightleftarrows N^*$	T(°C) $N\rightleftarrows I$ or $N^*\rightleftarrows I$
1	8CB	BDH		no	no		33.5	40.8
2	ZLI 3488 4-*n*-heptyl oxyphenyl	Meck home synthesized		yes	yes	61.0	66.0	85
3	4′-*n*-decyl oxybenzoate 4-[2-methyl butanoyloxy	home synthesized		no (achiral by compensation)	no	83.2	87.1	90.6
4	phenyl]4-decyl oxythiobenzoate] (racemic mixture)					72.7	74.6	76

We have controlled this point by an auxiliary run, the results of which are given in Fig. 6. As expected, in the range 28 °C–34 °C we find quite linear variations of $\ln I_{BW}(\tau_R;\tau_{pu};0)$ with τ_{pu}, leading to $\tau_{pu,1/2}$ close to 30 ps.

These reorientational times—a few tens of picoseconds— are in very good agreement with the ones obtained by other optical techniques [8,13,14] and QNS [9–11]. Basically, in a model of isotropic orientational diffusion, they are related to the $l=2$ spherical component of the spatially averaged orientation-dependent pair-correlation function. They must be interpreted as times describing rotational librations of individual molecules modified by short-range coupling to neighboring particles. In the models of rotational relaxation in dense media composed of rodlike molecules [40–42], such fast components of the relaxation are associated with reorientation of the rod within the cylinder formed by its nearest neighbors (pseudo-free-individual-reorientation). The models also include low components generated by the rotational diffusion of the cylinder (coupled rotations of some tens of particles), with associated times in the range of some hundred of picoseconds. These last times have been measured by FIR [11] from resonances near 150 cm^{-1}, i.e., 5×10^8 Hz, corresponding to the actual highest frequency accessible with the DS technique. Having checked the self-consistency of our results and their good agreement with other published investigations, we have explored the thermal behavior of I_{BW} within the three phases Sm-A, N, and I. Molecules show homeotropic orientation both in the Sm-A and N phases and random orientation in the I phase. Results are reported in Fig. 7. Two visual observations can be immediately pointed out.

(i) $I_{BW}(\tau_R;0;0)$ remains constant within each phase. This result is in perfect agreement with the measured intensity of the OKE signal in the picosecond range [14]; the measured linewidth of the OKE in the same range [14], and the integrated spectrum of the wings of RS [13]. It confirms the "pseudo" individual molecular origin of the effect.

(ii) There is no variation of the signal intensity at the Sm-$A\rightleftharpoons N$ transition, showing that probably both Γ_1^2 and τ_R do not markedly vary across this transition. On the other hand, I_{BW} increases by a factor close to 2.5 at the $N\rightarrow I$ transition.

This important increase could be due to the following factors: (a) Allowed rotations about all the axes in the I phase. In this case, the highest first-order polarizability (along the long molecular axis) plays a part that was forbidden in the Sm-A and N phases, increasing now the parameter A. (b) Lower reorientation times τ_R in the I phase, as already observed [13], and connected to the sudden decrease of the shear viscosity at the $N\rightarrow I$ transition [43].

C. Compound 2

Preliminary results have been already published [17]. The Merck ZLI 3488 is a ferroelectric mixture we selected because of its large cholesteric pitch (50 μm), which appears as the most important parameter in the alignment process. By surface treatment, use of a magnetic field, and repeated thermocycles in the vicinity of the Sm-$A\rightleftharpoons N^*$ phase transition, we have aligned two samples, 200-μm and 500-μm thick, having an optical quality similar to that obtained with 8CB. At the Sm-$A\rightarrow$Sm-C^* transition, the sample becomes opaque, allowing a visual observation and an unambiguous determination of the transition temperature. Figure 8 reports the results of this investigation (cooling and heating runs). We observe a decrease of $I_{BW}(\tau_R;0;0)$ in the last degree before the transition. Of course, we have carefully controlled, by visual observation, that the sample remains totally transparent down to the last experimental point. This observation suggests the presence of a pretransitional Sm-C^* effect in the vicinity of the transition. Such an

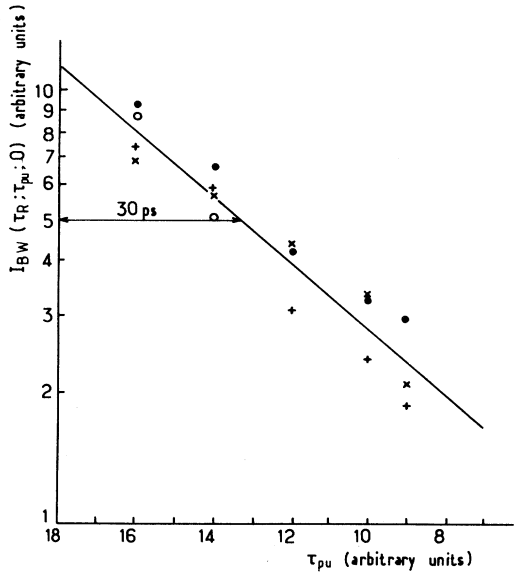

FIG. 6. Variation of $I(\tau_R;\tau_{pu};0)$ with the pump delay. compound, 8CB; thickness of the sample, 200 μm. ●, 28.1 °C; ×, 33.1 °C; +, 31.0 °C; ○, 33.6°C.

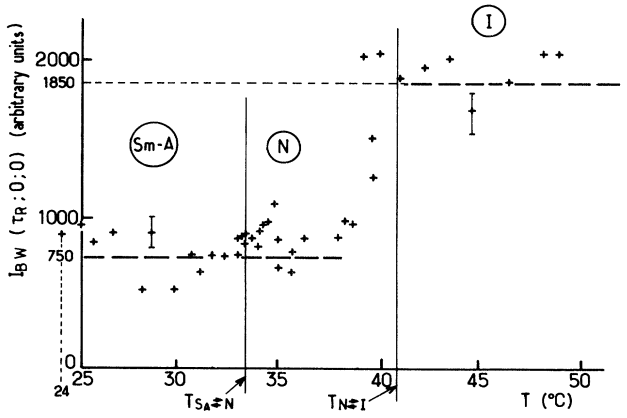

FIG. 7. Variation of the DFWM amplitude with temperature for 8CB; thickness of the sample, 200 μm.

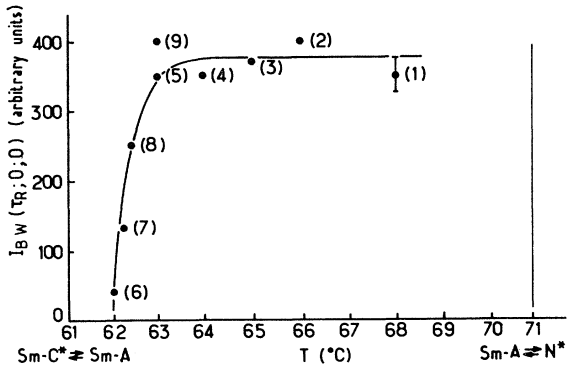

FIG. 8. DFWM amplitude vs temperature for the Merck Ferroelectric Liquid Crystal ZLI 3488 (Sm-A phase); thickness of the sample, 500 μm; $t_{\text{Sm-}C^*\rightleftharpoons\text{Sm-}A} \simeq 61.0\,^{\circ}\text{C}$; $t_{\text{Sm-}A\rightleftharpoons N^*} \simeq 71.0\,^{\circ}\text{C}$.

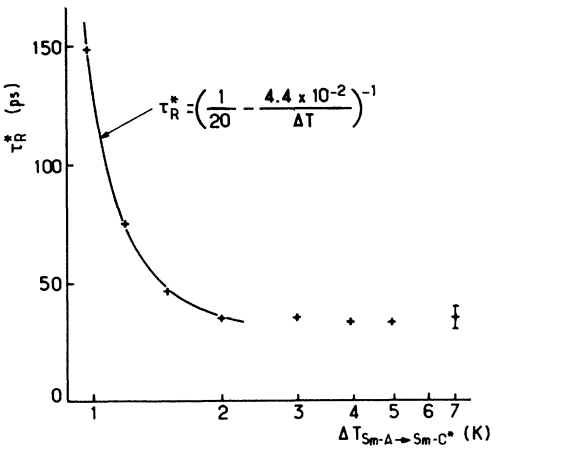

FIG. 9. Fit of the estimated τ_R^* to Eq. (9). Compound Merck ZLI 3488.

idea is supported by recent studies of the dynamics of ferroelectric liquid crystsls, showing fluctuations of a helical type well above the Sm-A–Sm-C^* transition, and by x-ray experiments where density modulations of both Sm-A and Sm-C^* are seen inside a wide (1 K) temperature range across the transition [44].

We can interpret this observation in two ways: (i) By a decrease of the "static" parameter A. However, we do not see any physical argument leading to such a behavior. (ii) More probably, by an increase of τ_R, i.e., a slowing down of the molecular reorientation about the long axis, in agreement with the widespread idea [45,46] of hindered rotation of the transverse component of the molecular dipole moment in the C^* ferroelectric phase. We must immediately state that we are dealing here with a slowing down in the Sm-A phase (τ_R is multiplied by 2 or 3) and not with a strong hindrance, only expected in Sm-C^* phases with permanent polarization. Obviously, the molecular rotation can only be slowed down in the Sm-A phases.

The observed effect can be explained [17] by a coupling between molecular fluctuating biaxiality polarization in the cybotactic groups formed in the Sm-A phase near the transition. By fluctuating polarization we mean reorientation of the individual transverse dipoles that cannot be directly probed by the laser field and that are known to have characteristic time about 3 τ_R. After coupling, Eq. (9) of Ref. [17] can be written

$$\tau_R^* = \left[\frac{1}{\tau_R} - \frac{B}{(T-T_C)^{\gamma}} \right]^{-1} . \tag{9}$$

τ_R is the characteristic time of the biaxial fluctuations without coupling to the polarization, B a coupling constant, and γ the critical exponent of the susceptibility. Figure 9 shows good agreement from evaluated τ_R (by use of Fig. 3) and calculated values from Eq. (9) with $\tau_R = 20$ ps; $B = 4.4 \times 10^{-2}$ ps^{-1} K and $\gamma = 1$ (mean-field approximation).

Recently, an alternative explanation of the observed effect has been proposed [47]. It is critically based on the existence of a Sm-C phase at lower temperature, inducing cybotactic groups in the Sm-A phase. Arguing that the DFWM experiment probes the reorientation of the in-plane director about the layer normal, the observed difference between chiral and achiral cases is attributed to a coupling between the tilt angle (modulus of the order parameter) and the in-plane director (phase) which should be allowed in the chiral case only. Such an alternative explanation seems unrealistic for two reasons: (i) as far as we know, when only one complex order parameter is involved, the phase must not be included in the free-energy expression, as has been done in Ref. [47]; (ii) the in-plane director cannot be defined in 8CB which has no Sm-C phase, and the proposed explanation does not seem to apply in the general case.

Very recently [48], a DS experiment has been performed on a nonoriented ferroelectric liquid crystal; this exhibits a frequency relaxation at 500 MHz showing no appreciable variations in a temperature range of about 25 K (from 10 K above the Sm-$A \rightarrow I$ transition down to the crystal). This is in contrast with the conclusions of previously published results obtained with the same DS technique [49]. This relaxation is assigned to the rotation of the mesogens around their long molecular axis, which is assumed to be free not only in the high-temperature phases but also all the way across the ferroelectric Sm-C^* one. Obviously, this experiment does not probe the *individual* molecular reorientation about the long axis and cannot be directly compared to our work.

D. Compounds 3 and 4

Compounds 3 and 4 have been studied to try to unambiguously establish the link between the observed decreases of I_{BW} of compound 3 and the pretransitional ferroelectric order in the Sm-A phase, close to the Sm-$A \rightleftharpoons$SM-C^* transition. Compound 3 is achiral and presents a Sm-C phase. Results are reported in Fig. 10. We do not see any decrease in the last degree (8 experimental points) of the Sm-A phase. Therefore, it is clear that a marked difference exists in this experiment between chiral and achiral compounds. At last, we have

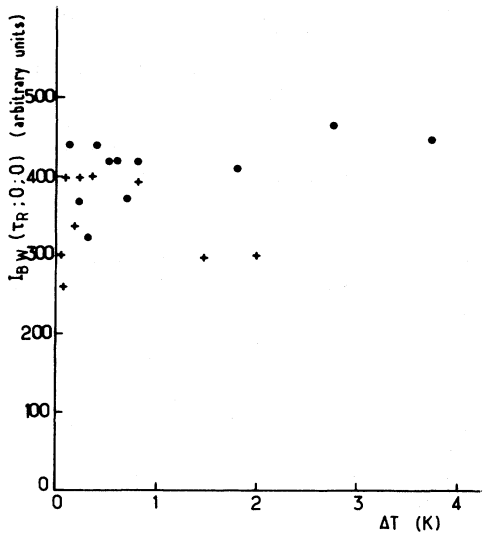

FIG. 10. DFWM amplitude vs $\Delta T = T - T_{AC}$ for compounds 3(●) and 4(+).

checked compound 4, which is a home-synthesized racemic binary mixture, in order to see if steric effects, due to the peculiar arrangement of the chiral tail, can be responsible for the slowing down of the rotation. Note that we now have $B = 0$ [Eq. (9)] and $\tau_R^* = \tau_R$. Figure 10 does not exhibit any decrease down to the phase transition, so the slowing down seems to be directly connected to the ferroelectric polarization and not due to steric molecular effects. Let us note here that recently published results do not definitely solve the problem of whether differences between chiral and racemic liquid crystals exist or not. Measurements of the heat capacity at constant pressure at the Sm-$A \rightarrow$Sm-C^* transition [50] do not reveal any difference in chiral and racemic 2-methylbutyl-4'-*n*-pentyloxy-biphenyl-4-carboxylate, although another experiment shows that it appears that the phase transition is weakly first order in a chiral compound and continuous in a racemic one near a tricritical point [51].

V. CONCLUSION

We have presented results of degenerate four-wave mixing on isotropic and homeotropic liquid crystals. In I phases, our results are equivalent to those obtained with ordinary liquids (CS_2), proving that we are dealing with individual reorientations. Signals monitored in N and Sm-A phases are attributed to individual molecular reorientations about the long molecular axis. The observed 1/2.5 decrease of the signal with respect to the isotropic case is due to a reduction of the degree of freedom. In chiral compounds, the slowing down of the reorientation (a factor of about 3 near the Sm-$A \rightarrow$Sm-C^* phase transition) is interpreted as being due to a coupling between the fluctuating polarization and the transient biaxial mode induced by the laser field. Achiral and racemic compounds do not present this behavior which seems directly connected to the vicinity of the ferroelectric Sm-C^* phase.

ACKNOWLEDGMENTS

We wish to thank B. Lemaire for valuable aid in the numerical calculations, J. C. Rouillon for technical assistance, and J. P. Parneix for helpful discussions.

[1] T. W. Stinson and J. D. Litster, Phys. Rev. Lett. **25**, 503 (1970).
[2] G. K. L. Wong and Y. R. Shen, Phys. Rev. Lett. **30**, 895 (1973).
[3] J. Prost and J. R. Lalanne, Phys. Rev. A **8**, 2090 (1973).
[4] G. K. L. Wong and Y. R. Shen, Phys. Rev. A **10**, 1277 (1974).
[5] J. R. Lalanne, Phys. Lett. **51A**, 74 (1975).
[6] P. G. DeGennes, Phys. Lett. **30A**, 454 (1969); Mol. Cryst. Liq. Cryst. **12**, 193 (1971).
[7] By "pseudoindividual" fluctuations, we mean fluctuations of individual molecules modified by coupling with neighboring particles (short-range order).
[8] J. A. Janik, M. Godlewska, T. Grochulski, A. Kocot, E. Sciesinska, J. Sciesinski, and W. Witko, Mol. Cryst. Liq. Cryst. **98**, 67 (1983).
[9] F. Volino, A. J. Dianoux, and A. Heideman, J. Phys. Lett. **40**, 583 (1979).
[10] A. J. Leadbetter, J. M. Richardson, and J. C. Frost, J. Phys. Colloq. **40**, 125 (1979).
[11] J. A. Janik, J. Krawczyk, J. M. Janik, and K. Otnes, J. Phys. Colloq. **40**, 169 (1979).
[12] A. Nayeem and J. H. Freed, J. Phys. Chem. **93**, 6539 (1989).
[13] N. M. Amer, Y. S. Lin, and Y. R. Shen, Solid State Commun. **16**, 1157 (1975).
[14] J. R. Lalanne, B. Martin, B. Pouligny, and S. Kielich, Opt. Commun. **19**, 440 (1976).
[15] G. Eyring and M. D. Fayer, J. Chem. Phys. **81**, 4314 (1984).
[16] P. A. Madden, F. C. Saunders, and A. M. Scott, IEEE J. Quantum Electron. **QE-22**, 1287 (1986).
[17] J. R. Lalanne, J. Buchert, C. Destrade, H. T. Nguyen, and J. P. Marcerou, Phys. Rev. Lett. **62**, 3046 (1989).
[18] B. I. Stepanov, E. V. Ivakin, and A. S. Rubanov, Dokl. Akad. Nauk **196**, 567 (1971) [Sov. Phys.—Dokl. **16**, 46 (1971)].
[19] J. Buchert, R. Dorsinville, P. Delfyett, S. Krimchansky, and R. R. Alfano, Opt. Commun. **52**, 433 (1985).
[20] G. Martin and R. W. Hellwarth, Appl. Phys. Lett. **34**, 371 (1979).
[21] W. M. Dennis, W. Blau and D. J. Bradley, Appl. Phys. Lett. **47**, 200 (1985).
[22] C. K. Wu, P. Agostini, G. Petite, and F. Fabre, Opt. Lett. **8**, 67 (1983).
[23] K. A. Nelson, R. J. D. Miller, D. R. Lutz, and M. D. Fayer, Phys. Rev. B **24**, 3261 (1981).
[24] A. Yariv, IEEE J. Quantum Electron. **QE-14**, 650 (1978).
[25] S. Kielich, Acta Phys. Polonica **30**, 683 (1966).
[26] The ansiotropy of the first-order polarizability is defined

by [25] $\Gamma^2=\frac{3}{2}[\mathrm{Tr}(\alpha\alpha)-\frac{1}{3}(\mathrm{Tr}\alpha)^2]$, where α is the first-order polarizability tensor.

[27] For wavelengths larger than 0.53μm, i.e., far from the electronic absorption resonances, the third-order polarizability χ describing the electronic deformation is about 10^{-36} esu for both CS_2 and benzene, and it contributes to about 5% of the OKE constant of CS_2. See B. F. Levine and C. G. Bethea, J. Chem. Phys. **63**, 2666 (1975).

[28] J. R. Lalanne, B. Lemaire, J. Rouch, C. Vaucamps, and A. Proutiere, J. Chem. Phys. **73**, 1927 (1980).

[29] M. J. Soileau, E. W. Van Stryland, S. Guha, E. J. Sharp, G. L. Wood, and J. L. W. Pohlmann, Mol. Cryst. Liq. Cryst. **143**, 139 (1987).

[30] M. J. Soileau, S. Guha, W. E. Williams, E. W. Van Stryland, and H. Vanherzeele, Mol. Cryst. Liq. Cryst. **127**, 321 (1985).

[31] A recent calculation on the cyanobiphenyl series, using Pariser, Parr, Pople or Huckel approximations [see R. Risser, D. W. Allender, M. A. Lee, and K. E. Schmidt, Mol. Cryst. Liq. Cryst. **179**, 335 (1990)] predicts the electronic contribution of the mean third-order polarizability to be about 10^{-33} esu in, i.e., of the same magnitude as that measured on very large molecules. The latter, like for instance β-carotene which has 11 conjugated double bonds, show broad delocalization of the π electrons over the whole chain [see J. P. Hermann, D. Ricard, and J. Ducuing, Appl. Phys. Lett. **23**, 178 (1973)]. Such high polarizabilities, when predicted for liquid-crystal molecules having only moderate conjugation in their central framework, seem to be unrealistic.

[32] D. Kivelson and P. A. Madden, Annu. Rev. Phys. Chem. **31**, 523 (1980).

[33] M. Boulanger (private communication).

[34] M. A. Vasil'eva, J. Vischakas, V. Kabelka, and A. V. Masalov, Opt. Commun. **53**, 412 (1985).

[35] Compound 4 has been prepared according to R. J. Twieg, K. Betterton, H. T. Nguyen, W. Tang, and W. Hinsberg, Ferroelectrics, **91**, 243 (1989), by using a commericial racemic 2-methylbutanoic acid.

[36] Rotations less than 5 arc min have been measured in DOBAMBC ($\lambda=442$ nm) for 100-μm-thick samples close to the Sm-$A\rightarrow$Sm-C^* phase transition. See E. I. Demikhov, V. K. Dolganov, and V. M. Filev, Pis'ma Zh. Eksp. Teor. Fiz. **37**, 305 (1983) [JETP Lett. **37**, 361 (1983)]. Recent work of P. J. Collings (private communication) shows rotations less than 13 arc min in similar conditions.

[37] J. R. Lalanne, J. Phys. (Paris) **30**, 643 (1969).

[38] E. P. Ippen and C. V. Shank, Appl. Phys. Lett. **26**, 92 (1975).

[39] ρ_{CS2} and n_{CS2} are taken from from *Handbook of Chemistry and Physics*, 64th ed., edited by R. C. Weast (CRC, Boca Raton, FL, 1984). Γ^2_{CS2} is taken from Ref. [37]. ρ_{8CB} is from D. A. Dunmur and W. H. Miller, J. Phys. (Paris) **40**, 471 (1978). n_{8CB} is taken from J. D. Bunning, D. A. Crellin, and T. E. Faber, Liq. Cryst. **1**, 37 (1986). $\Gamma^2_{I8CB}=441\times10^{-49}$ cm^6 is taken from Ref. [28] with the assumption that the C_8H_{17} chain has an isotropic first-order polarizability in a plane perpendicular to the long molecular axis.

[40] P. D. Maker, Phys. Rev. A **1**, 923 (1970).

[41] K. M. Zero and R. Pecora, Macromolecules **15**, 87 (1982).

[42] V. I. Gajduk and Y. P. Kalmykov, J. Chem. Soc. Faraday Trans. **2**, 929 (1981).

[43] P. Martinoty, S. Candau, and F. Debeauvais, Phys. Rev. Lett. **27**, 1123 (1971).

[44] C. W. Garland (private communication).

[45] R. B. Meyer, Mol. Cryst. Liq. Cryst. **40**, 33 (1977).

[46] L. A. Beresnev, E. P. Pozhidayev, and L. M. Blinov, Ferroelectrics **59**, 321 (1984); L. M. Blinov, *Electro-Optical and Magneto-Optical Properties of Liquid Crystals* (Wiley, New York, 1983).

[47] H. R. Brand and H. Pleiner, Phys. Rev. Lett. **64**, 1309 (1990).

[48] K. Kremer, S. U. Vallerien, H. Kapitza, R. Zentel, and E. W. Fisher, Phys. Rev. A **42**, 3667 (1990).

[49] L. Benguigui, J. Phys. (Paris) **43**, 915 (1982).

[50] S. C. Lien, C. C. Huang, and J. W. Goodby, Phys. Rev. A **29**, 1371 (1984).

[51] H. Y. Liu, C. C. Huang, C. Bahr, and G. Heppke, Phys. Rev. Lett. **61**, 345 (1988).